processes

Article

Tracking Control of X-Z Inverted Pendulum with Block Backstepping

Zhuang-Zhuang Xin and Jia-Jun Wang *

School of Automation, Hangzhou Dianzi University, Hangzhou 310018, China; xinzhuangzhuang@hdu.edu.cn
* Correspondence: wangjiajun@hdu.edu.cn

Abstract: As the extension of traditional linear (or X) inverted pendulum (IP), X-Z IP is a multiple-input multiple-output (MIMO), underactuated, open-loop unstable, and nonlinear system. In the tracking control of the X-Z IP, the equilibrium point changes with the pivot position of the pendulum. This makes linear control theories have difficulties in realization of the tracking control for the pendulum. The underactuated feature of the pendulum makes the feedback linearization unsuitable to simplify the control design. With the present model of the X-Z IP, there is no way to realize the backstepping design. This paper gives a novel state transformation method for the X-Z IP. Through the state transformation, the block backstepping can be easily deployed in the controller design of the X-Z IP. The proposed controller can achieve the tracking control in the vertical plane. Simulation results certify the rightness and effectiveness of the proposed tracking controller.

Keywords: X-Z inverted pendulum; block backstepping; zero dynamics; tracking control

check for updates

Citation: Xin, Z.-Z.; Wang, J.-J. Tracking Control of X-Z Inverted Pendulum with Block Backstepping. *Processes* **2021**, *9*, 1138. https://doi.org/10.3390/pr9071138

Academic Editor: Mohd Azlan Hussain

Received: 29 May 2021
Accepted: 28 June 2021
Published: 30 June 2021

1. Introduction

The traditional linear inverted pendulum (IP), which can also be called X IP, is a typical test platform for different control strategies and is widely used by the researchers. As we know from the literature, before 2000, the research studies on the IP were mainly concentrated on the X IP. In 2000, the motion space of the IP was extended to the horizontal plane [1,2]. The proposed IP can be called planar (X-Y) IP. In 2004, the motion space of the IP was further extended to the vertical plane [3,4]. And the proposed IP can be called X-Z IP. The X-Y or X-Z IP has more control forces and controlled variables. There exist more difficulties in the control of the X-Y or X-Z IP than that of the X IP. This brief paper mainly concentrates on the controller design for the X-Z IP.

According to the present literature, the control of the IP can be divided into swinging-up control, stabilization and tracking control. As one important aspect of the X IP control, the swinging-up of the X IP can be realized with many strategies, such as energy control [5], the energy speed gradient method [6], and time optimal method [7,8]. The stabilization of the IP is the basic requirement in the control of the IP. Almost global or semi-global stabilization [9,10], global stabilization [11–13], and stabilization with uncertainties [14] were achieved one after another. Stabilization is a special case of the tracking control. The tracking control of the X-Y or X-Z IP control is still a challenging task. In this paper, we do not consider the problem of swinging up of the pendulum and, rather, assume that initial conditions are located in the upper hemisphere.

At present, only a few examples of literature can be found that concentrated on the tracking control of the X-Y or X-Z IP. The nonlinear stable inversion-based output tracking control was firstly applied in the control of the X-Y IP [15], where the feedback is linear, which make the domain of attraction limited. In References [16,17], three PID controllers were applied in the tracking control of the X-Z IP. The parameter tuning of the PID controllers is not an easy task even for an experienced researcher. In Reference [18], the sliding–mode control was used to design the tracking controller for the X-Z IP. The control error was related with the desired trajectory. In Reference [19], the tracking control was successfully realized with the flatness based active disturbance rejection control. The adoption of linearizing the system around an equilibrium limited the convergence range of the pendulum. According to the present literature as far as we know, there is no report on the tracking control of the X-Z IP with block backstepping.

Backstepping is a systematic and recursive design methodology for nonlinear feedback control [20,21]. The most appealing point of backstepping is to use the virtual control variable to make the original high-order system simple, and the controller can be derived step by step. In the controller design, the backstepping requires that the control system under consideration is in the strict feedback form. For the MIMO system, the strict feedback form often can not be satisfied. Block backstepping is a novel backstepping design method and has become one of the most efficient backstepping control strategy to deal with the problems of nonlinear MIMO systems [22,23]. In this paper, the block backstepping will be adopted to solve the tracking control problem for the X-Z IP.

The remainder of this paper is organized as following five sections. Section 2 presents the state transformation of the X-Z IP. Section 3 demonstrates tracking controller design for the X-Z IP with the block backstepping. Section 4 illustrates the simulation results of the tracking control. Section 5 gives some discussions. At last, a brief conclusion is summarized in Section 6.

2. State Transformation

The X-Z IP on a pivot driven by one horizontal force F_x and one vertical force F_z is shown in Figure 1. The X-Z IP can move in a plane perpendicular to X-Z. The state equations of the X-Z IP are given as [13,18]

$$\ddot{x} = \frac{Mml\dot{\theta}^2 \sin\theta + (M + m\cos^2\theta)F_x - mF_z \sin\theta\cos\theta}{M(M+m)}, \quad (1)$$

$$\ddot{z} = \frac{Mml\dot{\theta}^2 \cos\theta - mF_x \sin\theta\cos\theta + (M + m\sin^2\theta)F_z - M(M+m)g}{M(M+m)}, \quad (2)$$

$$\ddot{\theta} = \frac{-F_x\cos\theta + F_z\sin\theta}{Ml}, \quad (3)$$

where (x,z), $(\dot{x},\dot{z})$, $(\ddot{x},\ddot{z})$ are the position, speed, acceleration of the pivot in the xoz coordinate system, respectively, l is the distance from the pivot to the center of mass of the pendulum, M and m are the mass of the pivot and the pendulum, respectively, g is the acceleration constant due to gravity, F_x is the horizontal force, and F_z is the vertical force. We assume that $-1\ \text{m} \le x \le 1\ \text{m}$, $-1\ \text{m} \le z \le 1\ \text{m}$, and the inertia of the pendulum is negligible. Here, m is the meter.

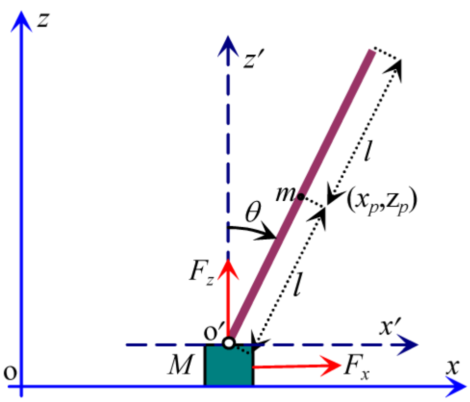

Figure 1. The structure of the X-Z IP.

To apply the block backstepping, the state transformation of the X-Z IP can be achieved with the following seven steps.

Step 1: Redefining $e_x = x - x_d$, $e_z = z - z_d$, where x_d and z_d are the desired signals, we assume that x_d and z_d are no less than three times differentiable. Then, the state Equations (1)–(3) can be rewritten as

$$\ddot{e}_x = \frac{Mml\dot{\theta}^2 \sin\theta + (M + m\cos^2\theta)F_x - mF_z \sin\theta\cos\theta - M(M+m)\ddot{x}_d}{M(M+m)}, \tag{4}$$

$$\ddot{e}_z = \frac{Mml\dot{\theta}^2 \cos\theta - mF_x \sin\theta\cos\theta + (M + m\sin^2\theta)F_z - M(M+m)(g+\ddot{z}_d)}{M(M+m)}, \tag{5}$$

$$\ddot{\theta} = \frac{-F_x\cos\theta + F_z\sin\theta}{Ml}. \tag{6}$$

Step 2: Redefining $e_{xp} = e_x + l\sin\theta$ and $e_{zp} = e_z + l(\cos\theta - 1)$, we can obtain that $\dot{e}_{xp} = \dot{e}_x + l\dot{\theta}\cos\theta$, $\dot{e}_{zp} = \dot{e}_z - l\dot{\theta}\sin\theta$. Then, $\ddot{e}_{xp} = \ddot{e}_x + l\ddot{\theta}\cos\theta - l\dot{\theta}^2\sin\theta$ and $\ddot{e}_{zp} = \ddot{e}_z - l\ddot{\theta}\sin\theta - l\dot{\theta}^2\cos\theta$ can be acquired. Using the redefined e_{xp} and e_{zp}, we can obtain the following equations:

$$\ddot{e}_{xp} = \frac{F_x\sin^2\theta + F_z\sin\theta\cos\theta - Ml\dot{\theta}^2\sin\theta}{M+m} - \ddot{x}_d, \tag{7}$$

$$\ddot{e}_{zp} = \frac{F_x\sin\theta\cos\theta + F_z\cos^2\theta - Ml\dot{\theta}^2\cos\theta}{M+m} - g - \ddot{z}_d, \tag{8}$$

$$\ddot{\theta} = \frac{-F_x\cos\theta + F_z\sin\theta}{Ml}. \tag{9}$$

Step 3: Redefining $e_{xm} = -e_{xp}$, $e_{zm} = e_{zp}$, $u_{xz} = (F_x\sin\theta + F_z\cos\theta)/(M+m)$ and $u_\theta = (-F_x\cos\theta + F_z\sin\theta)/(Ml)$, based on (7)–(9), we can obtain the following equations:

$$\ddot{e}_{xm} = -u_{xz}\sin\theta + \frac{M}{M+m}l\dot{\theta}^2\sin\theta + \ddot{x}_d, \tag{10}$$

$$\ddot{e}_{zm} = u_{xz}\cos\theta - \frac{M}{M+m}l\dot{\theta}^2\cos\theta - g - \ddot{z}_d, \tag{11}$$

$$\ddot{\theta} = u_\theta. \tag{12}$$

From the definition of the u_{xz} and u_θ, the actual control forces F_x and F_z can be obtained as the following equations:

$$F_x = (M+m)u_{xz}\sin\theta - Mlu_\theta\cos\theta, \tag{13}$$

$$F_z = (M+m)u_{xz}\cos\theta + Mlu_\theta\sin\theta. \tag{14}$$

Step 4: Redefining $u_m = u_{xz} - \frac{M}{M+m}l\dot{\theta}^2$, based on (10)–(12), we can obtain the following equations:

$$\ddot{e}_{xm} = -u_m\sin\theta + \ddot{x}_d, \tag{15}$$

$$\ddot{e}_{zm} = u_m\cos\theta - g - \ddot{z}_d, \tag{16}$$

$$\ddot{\theta} = u_\theta. \tag{17}$$

Step 5: Redefining $e_a = e_{xm} + \sin\theta$, $e_b = e_{zm} - (\cos\theta - 1)$, $u_a = u_m + \dot{\theta}^2$, and $u_b = u_\theta$, based on (15)–(17), we can obtain the following equations:

$$\ddot{e}_a = -u_a\sin\theta + u_b\cos\theta + \ddot{x}_d, \tag{18}$$

$$\ddot{e}_b = u_a\cos\theta + u_b\sin\theta - g - \ddot{z}_d, \tag{19}$$

$$\ddot{\theta} = u_b. \tag{20}$$

Step 6: Let the control u_a and u_b be the following forms:

$$u_a = -(v_1 - \ddot{x}_d)\sin\theta + (v_2 + g + \ddot{z}_d)\cos\theta, \tag{21}$$

$$u_b = (v_1 - \ddot{x}_d)\cos\theta + (v_2 + g + \ddot{z}_d)\sin\theta. \tag{22}$$

With (18)–(22), the following equations can be obtained:

$$\ddot{e}_a = v_1, \tag{23}$$

$$\ddot{e}_b = v_2, \tag{24}$$

$$\ddot{\theta} = v_1\cos\theta + v_2\sin\theta - \ddot{x}_d\cos\theta + \ddot{z}_d\sin\theta + g\sin\theta. \tag{25}$$

Step 7: Let $\boldsymbol{\xi_1}$=$[\xi_{11}\ \ \xi_{12}]^T$=$[e_a\ \ e_b]^T$, where T represents the transpose. Similarly, let $\boldsymbol{\xi_2}$=$[\xi_{21}\ \ \xi_{22}]^T$=$[\dot{e}_a\ \ \dot{e}_b]^T$. And, at same time, let $\xi_3 = \theta$ and $\dot{\xi}_3 = \xi_4$. Then, we can obtain the following block model of the X-Z IP:

$$\dot{\boldsymbol{\xi}}_1 = \boldsymbol{\xi_2}, \tag{26}$$

$$\dot{\boldsymbol{\xi}}_2 = \boldsymbol{v}, \tag{27}$$

$$\dot{\xi}_3 = \xi_4, \tag{28}$$

$$\dot{\xi}_4 = f + \boldsymbol{bv}, \tag{29}$$

where $f = -\ddot{x}_d\cos\xi_3 + \ddot{z}_d\sin\xi_3 + g\sin\xi_3$, $\boldsymbol{b} = [b_1\ \ \ b_2]$=$[\cos\xi_3\ \sin\xi_3]$, and $\boldsymbol{v} = [v_1\ \ v_2]^T$.

Through the above state transformation with seven steps, the model of the X-Z IP is simplified to be the block state Equations (26)–(29) will be used for the block backstepping control design in the next section.

Remark 1. *In this paper, the boldface variables represent the matrices or vectors.*

3. Block Backstepping Design

3.1. Controller Design

Although the model of the X-Z IP has been transformed to the block state equations, (26)–(29) are still not the strict feedback form. The block backstepping can not be applied directly with (26)–(29). In the following, we will adopt the state transformation method proposed in Rudra [23,24] to achieve the design of the strict feedback form.

The block backstepping controller design for the X-Z IP can be realized with the following four steps.

Step 1: We select the first new state variable $\boldsymbol{\zeta}_1$ with the state variables in (26)–(29) and $\boldsymbol{\zeta}_1$ is given as

$$\boldsymbol{\zeta}_1 = \boldsymbol{\xi}_1 - \boldsymbol{K}(\xi_3 + \xi_4 - \boldsymbol{b}\boldsymbol{\xi_2}), \tag{30}$$

where $\boldsymbol{K} = [k_1\ \ k_2]^T$ is a constant column vector, which should make the state variables of the system stable and will be explained in the later section.

The derivative versus time of $\boldsymbol{\zeta}_1$ can be computed with the following expression:

$$\dot{\boldsymbol{\zeta}}_1 = \boldsymbol{\xi}_2 - \boldsymbol{K}(\xi_4 + f - \frac{d\boldsymbol{b}}{dt}\boldsymbol{\xi}_2), \tag{31}$$

where $\frac{d\boldsymbol{b}}{dt}$ represents the derivative versus time of $\boldsymbol{b}$, and $\frac{d\boldsymbol{b}}{dt} = [\frac{db_1}{dt}\ \ \frac{db_2}{dt}] = [-\xi_4\sin\xi_3\ \ \xi_4\cos\xi_3]$.

Step 2: According to the design of block backstepping, we can select the virtual control α as

$$\boldsymbol{\alpha} = -c_1\boldsymbol{\zeta}_1 - \lambda\int_0^t \boldsymbol{\zeta}_1 d\tau + \boldsymbol{K}(\xi_4 + f - \frac{d\boldsymbol{b}}{dt}\boldsymbol{\xi}_2), \tag{32}$$

where c_1 and λ are all positive constant.

Step 3: A new state variable is designed as $\boldsymbol{\zeta}_2 = \boldsymbol{\xi}_2 - \boldsymbol{\alpha}$. If we bring $\boldsymbol{\xi}_2 = \boldsymbol{\zeta}_2 + \boldsymbol{\alpha}$ into (31), then (31) can be rewritten as

$$\dot{\boldsymbol{\zeta}}_1 = -c_1\boldsymbol{\zeta}_1 - \lambda \int_0^t \boldsymbol{\zeta}_1 d\tau + \boldsymbol{\zeta}_2. \tag{33}$$

The derivative versus time of $\boldsymbol{\zeta}_2$ can be given as

$$\begin{aligned}\dot{\boldsymbol{\zeta}}_2 &= \dot{\boldsymbol{\xi}}_2 - \dot{\boldsymbol{\alpha}} \\ &= \boldsymbol{v} - [-c_1(-c_1\boldsymbol{\zeta}_1 - \lambda \textstyle\int_0^t \boldsymbol{\zeta}_1 d\tau + \boldsymbol{\zeta}_2) \\ &\quad -\lambda\boldsymbol{\zeta}_1 + \boldsymbol{K}(f + \boldsymbol{bv} + \tfrac{df}{dt} - \tfrac{d\boldsymbol{b}}{dt}\boldsymbol{v} - \tfrac{d^2\boldsymbol{b}}{dt^2}\boldsymbol{\xi}_2)],\end{aligned} \tag{34}$$

where $\frac{df}{dt} = -x_d^{(3)} \cos \xi_3 + \ddot{x}_d\xi_4 \sin \xi_3 + z_d^{(3)} \sin \xi_3 + \ddot{z}_d\xi_4 \cos \xi_3 + g\xi_4 \cos \xi_3$ and $\frac{d^2\boldsymbol{b}}{dt^2} = [-\xi_4^2 \cos \xi_3 - (f + \boldsymbol{bv}) \sin \xi_3 - \xi_4^2 \sin \xi_3 + (f + \boldsymbol{bv}) \cos \xi_3]$.

Equation (34) can be simplified as the following expression:

$$\dot{\boldsymbol{\zeta}}_2 = \boldsymbol{D}\boldsymbol{v} + \boldsymbol{\Phi}, \tag{35}$$

where $\boldsymbol{D}$ and $\boldsymbol{\Phi}$ are matrixes and are given as

$$\boldsymbol{D} = \boldsymbol{I} - \boldsymbol{K}\boldsymbol{B}, \tag{36}$$

$$\boldsymbol{\Phi} = (-c_1^2 + \lambda)\boldsymbol{\zeta}_1 + c_1\boldsymbol{\zeta}_2 - c_1\lambda \int_0^t \boldsymbol{\zeta}_1 d\tau - \boldsymbol{N}, \tag{37}$$

where

$$\boldsymbol{N} = \boldsymbol{K}(f + \frac{df}{dt} + N_0). \tag{38}$$

In (36), $\boldsymbol{I}$ is 2×2 identity matrix, and $\boldsymbol{B} = [B_1 \;\; B_2]$. B_1, B_2, and N_0 are given as

$$B_1 = \cos \xi_3 + \xi_4 \sin \xi_3 + \xi_{21} \sin \xi_3 \cos \xi_3 - \xi_{22} \cos^2 \xi_3, \tag{39}$$

$$B_2 = \sin \xi_3 - \xi_4 \cos \xi_3 + \xi_{21} \sin^2 \xi_3 - \xi_{22} \sin \xi_3 \cos \xi_3, \tag{40}$$

$$N_0 = \xi_4^2\xi_{21} \cos \xi_3 + f\xi_{21} \sin \xi_3 + \xi_4^2\xi_{22} \sin \xi_3 - f\xi_{22} \cos \xi_3. \tag{41}$$

Step 4: With (34), if we assume that the derivative versus time of ζ_2 satisfy the following equation:

$$\dot{\boldsymbol{\zeta}}_2 = -\boldsymbol{\zeta}_1 - c_2\boldsymbol{\zeta}_2, \tag{42}$$

then the control $\boldsymbol{v}$ can be acquired with (34) and (42) as

$$\boldsymbol{v} = \boldsymbol{D}^{-1}(-\boldsymbol{\Phi} - \boldsymbol{\zeta}_1 - c_2\boldsymbol{\zeta}_2), \tag{43}$$

where $\boldsymbol{D}^{-1}$ is the inverse matrix of $\boldsymbol{D}$.

According to the above control design, the control $\boldsymbol{v}$ in (43) can make the control system with new state variables $\boldsymbol{\zeta}_1$ and $\boldsymbol{\zeta}_2$ transform to the following forms:

$$\dot{\boldsymbol{\zeta}}_1 = -c_1\boldsymbol{\zeta}_1 - \lambda \int_0^t \boldsymbol{\zeta}_1 d\tau + \boldsymbol{\zeta}_2. \tag{44}$$

$$\dot{\boldsymbol{\zeta}}_2 = -\boldsymbol{\zeta}_1 - c_2\boldsymbol{\zeta}_2. \tag{45}$$

It is an easy job to prove that the variables $\boldsymbol{\zeta}_1$ and $\boldsymbol{\zeta}_2$ are globally asymptotic stable. And the proof can be referenced in Rudra [23,24].

3.2. *The Analysis of System Zero Dynamics*

In the above design, the controller shown in (43) can ensure that the stability of the state variables $\boldsymbol{\zeta}_1$ and $\boldsymbol{\zeta}_2$. Although the variables $\boldsymbol{\zeta}_1$ and $\boldsymbol{\zeta}_2$ of the reduced order model are composed with $\boldsymbol{\xi}_1$, $\boldsymbol{\xi}_2$, ξ_3, and ξ_4, we can not directly say that the variables $\boldsymbol{\xi}_1$, $\boldsymbol{\xi}_2$, ξ_3, and

ξ_4 are all stable. In the following, we will demonstrate that the controller shown in (43) can also ensure that the state variables $\boldsymbol{\zeta}_1$, $\boldsymbol{\zeta}_2$, ξ_3, and ξ_4 are stable through indirect method.

From the above design, it can be seen that the system with (31) and (35) is the reduced order model of the X-Z IP. The reduced order model with the states $\boldsymbol{\zeta_1}$ and $\boldsymbol{\zeta_2}$ is a four-order system. If the control $\boldsymbol{v}$ is substituted into (29), then (28) and (29) can be seen as the zero dynamics of the reduced order system. The relationship between the reduced order system and the simplified block system is given in Figure 2. In order to ensure the global asymptotic stability of the proposed controller, the zero dynamics of the reduced order system should be stabilized [25]. And if the zero dynamics is stable, the designed controller in (43) can make the whole system stable. Now, the stabilization of the zero dynamics is analyzed in the following part.

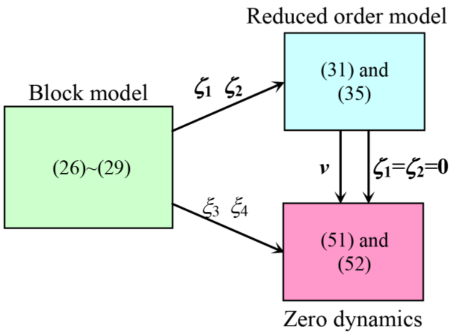

Figure 2. The decomposition of the block model.

The concrete zero dynamics of the reduced order system can be acquired through three steps.

Step 1: When the reduced order system is stable, then we can achieve $\zeta_1 = 0$ and $\dot{\zeta}_1 = 0$. With (31), the variable ξ_{21} and ξ_{22} can be computed with the following expressions:

$$\xi_{21} = \frac{k_1(\xi_4 + f)}{1 + k_1\xi_4 \sin\xi_3 - k_2\xi_4 \cos\xi_3}, \tag{46}$$

$$\xi_{22} = \frac{k_2(\xi_4 + f)}{1 + k_1\xi_4 \sin\xi_3 - k_2\xi_4 \cos\xi_3}. \tag{47}$$

Step 2: Substituting ξ_{21} and ξ_{22} in B_1, B_2, and N_0 with (46) and (47), B_1, B_2 and N_0 can be rewritten as

$$B_1 = \cos\xi_3 + \xi_4 \sin\xi_3 + \frac{(k_1 \sin\xi_3 \cos\xi_3 - k_2 \cos^2\xi_3)(\xi_4 + f)}{1 + k_1\xi_4 \sin\xi_3 - k_2\xi_4 \cos\xi_3}, \tag{48}$$

$$B_2 = \sin\xi_3 - \xi_4 \cos\xi_3 + \frac{(k_1 \sin^2\xi_3 - k_2 \sin\xi_3 \cos\xi_3)(\xi_4 + f)}{1 + k_1\xi_4 \sin\xi_3 - k_2\xi_4 \cos\xi_3}, \tag{49}$$

$$N_0 = \frac{(\xi_4^2 k_1 \cos\xi_3 + f k_1 \sin\xi_3 + \xi_4^2 k_2 \sin\xi_3 - f k_2 \cos\xi_3)(\xi_4 + f)}{1 + k_1\xi_4 \sin\xi_3 - k_2\xi_4 \cos\xi_3}. \tag{50}$$

Step 3: Substituting B_1, B_2, and N_0 in (48)–(50) into (36)–(38), further, with $\zeta_1 = 0$ and $\zeta_2 = 0$, we can obtain the zero dynamics as the following expressions:

$$\dot{\xi}_3 = \xi_4, \tag{51}$$

$$\dot{\xi}_4 = f + \frac{k_1 b_1 + k_2 b_2}{1 - k_1 B_1 - k_2 B_2}\left(f + \frac{df}{dt} + N_0\right). \tag{52}$$

Because f, b_1, b_2, B_1, B_2, $\frac{df}{dt}$, and N_0 are all trigonometric functions, the direct analysis of zero dynamics is very difficult. Now, we will analyze the zero dynamics with the help of phase portrait.

From the zero dynamics equation in (51) and (52), we can see that the phase portrait of the zero dynamics is relation with four variables, which are k_1, k_2, x_d, and z_d. Through the selection of k_1 and k_2, we can regulate the performance of the zero dynamics. To plot the phase portrait of zero dynamics, we need to know the desired tracking trajectory and the initial point. The desired tracking trajectory for the X-Z IP is a space eight-shape curve, which is given as following expressions with the period of 40 s,

$$x_d = 0.3\sin(0.1\pi t), \quad 0 \le t < 40, \tag{53}$$

$$z_d = \begin{cases} -0.3 - 0.3\cos(0.1\pi t), & 0 \le t < 10, \\ 0.3 - 0.3\cos(0.1\pi t), & 10 \le t < 20, \\ 0.3 + 0.3\cos(0.1\pi t), & 20 \le t < 30, \\ -0.3 + 0.3\cos(0.1\pi t), & 30 \le t < 40. \end{cases} \tag{54}$$

The initialization data are given as $x(0) = 0$, $z(0) = -0.3$ m, and $\theta(0) = \frac{\pi}{6}$ rad. The parameters of the X-Z IP are given in Table 1.

Table 1. Parameters of the X-Z inverted pendulum.

M **(kg)**	***m*** **(kg)**	***l*** **(m)**	***g*** **(m/s^2)**
1	0.1	0.5	9.8

To analyze the effect of k_1 to the zero dynamics, we first set $k_2 = 1$, the phase portrait of the zero dynamics is demonstrated in Figure 3a. Comparatively, to analyze the effect of k_2 to the zero dynamics, we set $k_1 = 8$, the phase portrait of the zero dynamics is demonstrated in Figure 3b.

From the phase portraits of the zero dynamics in Figure 3a,b, we can see that the controller in (43) can make the block control system stable. Then, we can conclude that the controller can also make the control of the X-Z IP stable.

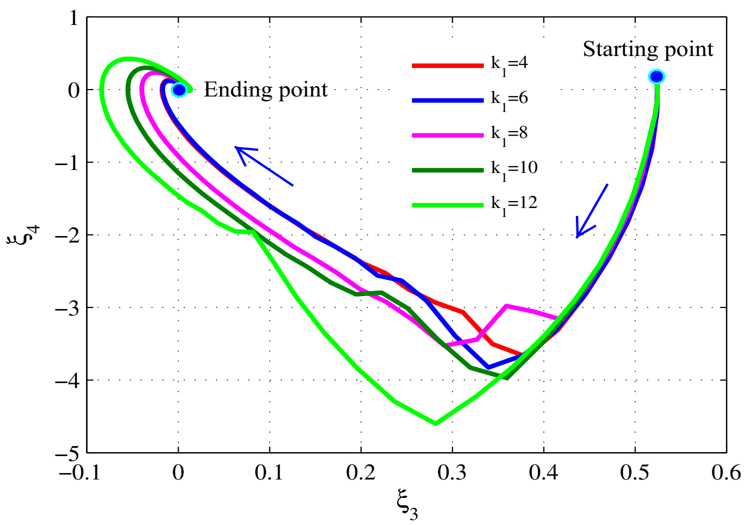

(**a**)

Figure 3. *Cont.*

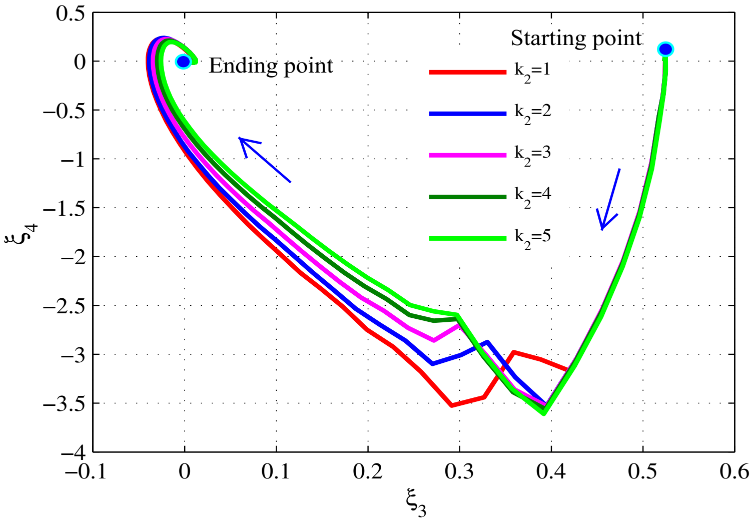

(**b**)

Figure 3. The phase portraits of the zero dynamics with different control parameters. (**a**) $k_2 = 1$; and (**b**) $k_1 = 8$.

4. Simulation

The control structure of the X-Z IP is shown in Figure 4.

We assume that control forces satisfy $|F_x| \leq 30$ N and $|F_z| \leq 30$ N of force is added. To track the desired trajectories that are given in (53) and (54), the control parameters of the controller are given in Table 2. The state variables are shown in Figure 5. The control errors are illustrated in Figure 6. And part controls in the transformation are shown in Figure 7. The trajectory tracking result of the X-Z IP is given in Figure 8.

Table 2. Parameters of the tracking controller.

c_1	c_2	λ	k_1	k_2
12	200	15	8	1

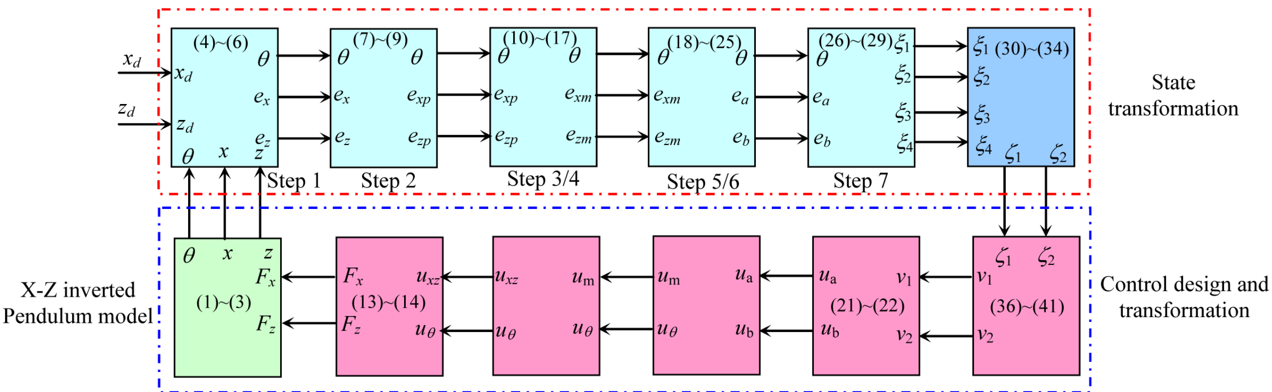

Figure 4. The control structure of the X-Z IP.

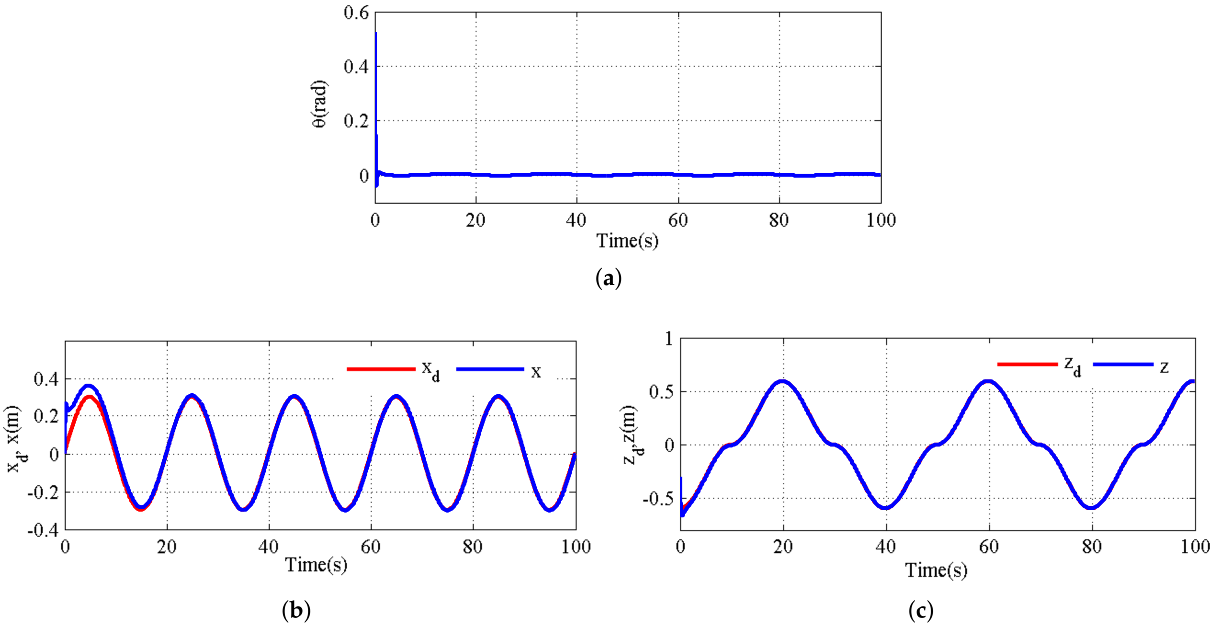

Figure 5. The state variables. (**a**) The angle θ; (**b**) the desired x_d and x; and (**c**) the desired z_d and z.

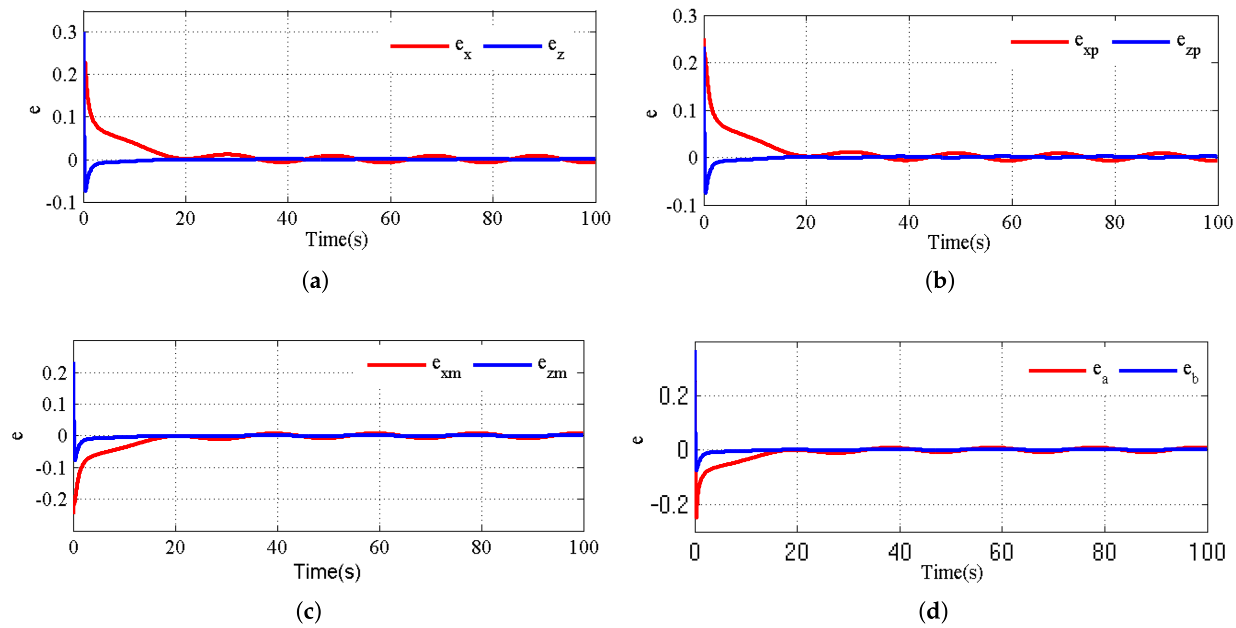

Figure 6. The control errors. (**a**) The errors e_x and e_z; (**b**) the errors e_{xp} and e_{zp}; (**c**) the errors e_{xm} and e_{zm}; and (**d**) the errors e_a and e_b.

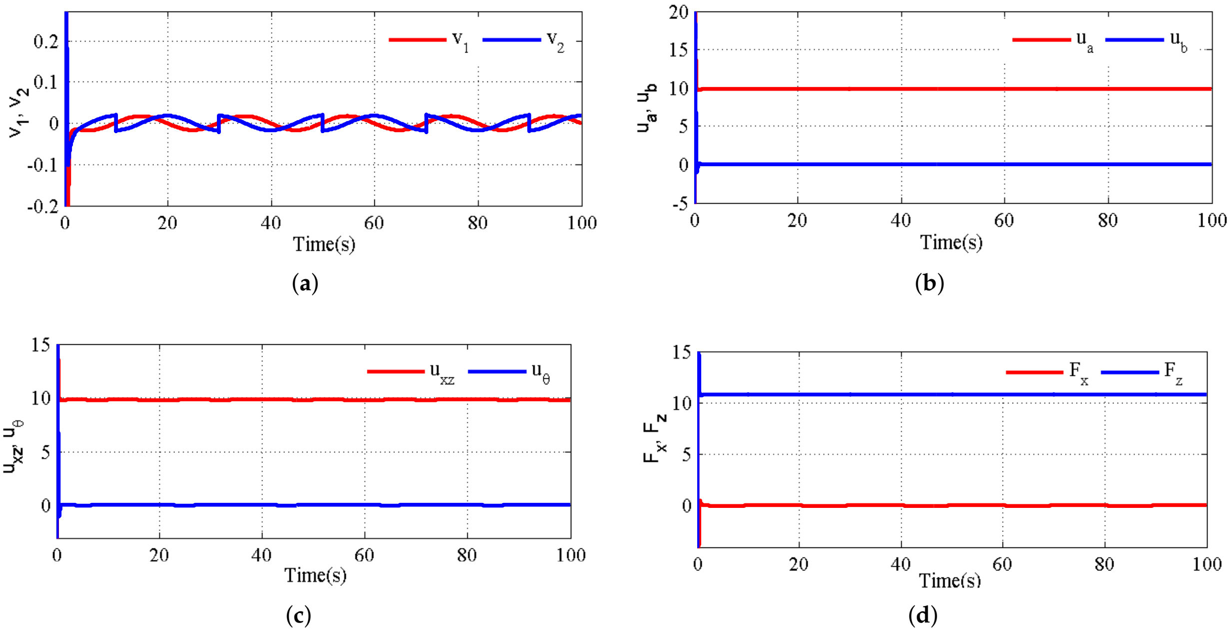

Figure 7. The control variables. (**a**) The control variables v_1 and v_2; (**b**) the control variables u_a and u_b; (**c**) the control variables u_{xz} and u_θ; and (**d**) the control variables F_x and F_z.

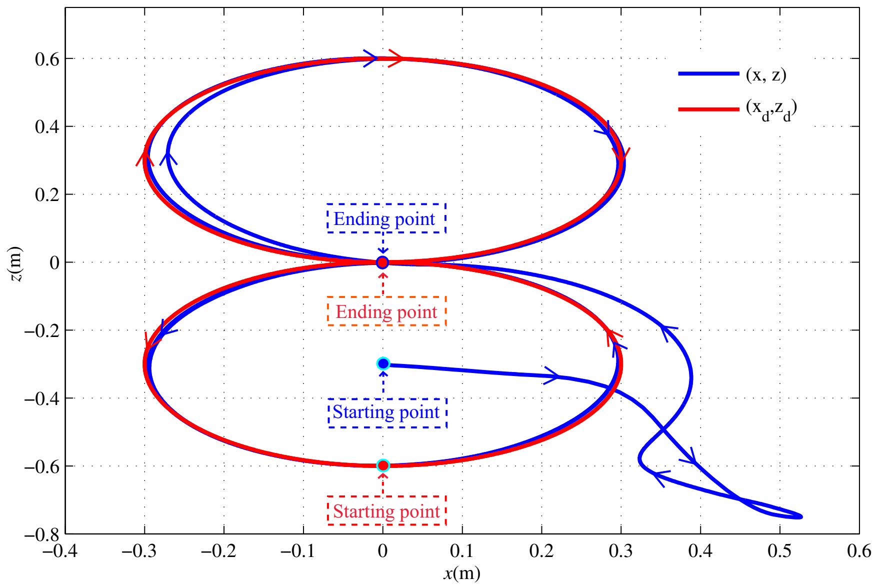

Figure 8. The trajectory tracking of the X-Z inverted pendulum.

To analyze the robustness of the proposed controller, some simulation tests are given and explained in the following. The robustness of the controller mainly includes system parameter uncertainties and external disturbances. In the proposed controller, the parameter uncertainties are reflected in M, m, and l, and the external disturbances are reflected in F_x, F_z, θ, x, and z. The changes of F_x, F_z, θ, x, and z by disturbances are represented by ΔF_x, ΔF_z, $\Delta\theta$, Δx, and Δz.

In order to test the robustness of the controller to different types of disturbance signals, a sine wave signal with an amplitude of $\Delta F_{x(z)}$ and a frequency of 20 Hz is used for the disturbance of $F_{x(z)}$, and a pulse signal with an amplitude of $\Delta\theta(\Delta x$ or $\Delta z)$ is used for the disturbance of $\theta(x$ or $z)$. The effects of changing the system parameters M, m, and l on θ, x, and z are shown in Figures 9–11, respectively. The effects of adding external disturbances ΔF_x, ΔF_z, $\Delta\theta$, Δx, and Δz on θ, x, and z are shown in Figures 12–16, respectively.

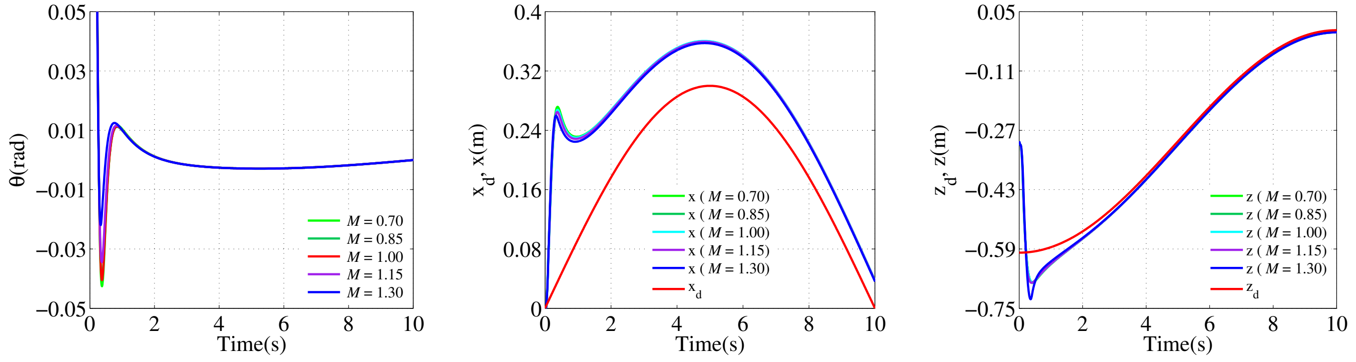

(**a**) (**b**) (**c**)

Figure 9. The simulation tests when $M = 0.70, 0.85, 1.00, 1.15$, and 1.30. (**a**) The θ; (**b**) the x_d and x; and (**c**) the z_d and z.

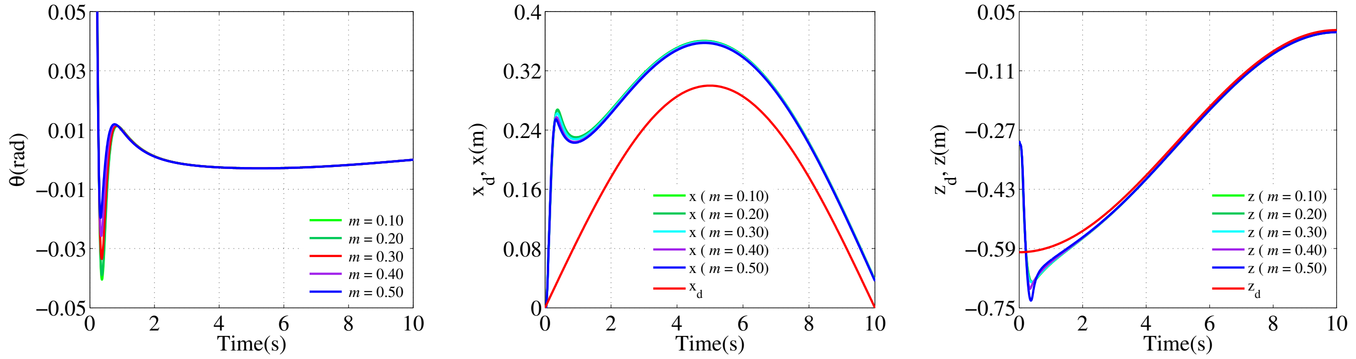

(**a**) (**b**) (**c**)

Figure 10. The simulation tests when $m = 0.10, 0.20, 0.30, 0.40$, and 0.50. (**a**) The θ; (**b**) the x_d and x; and (**c**) the z_d and z.

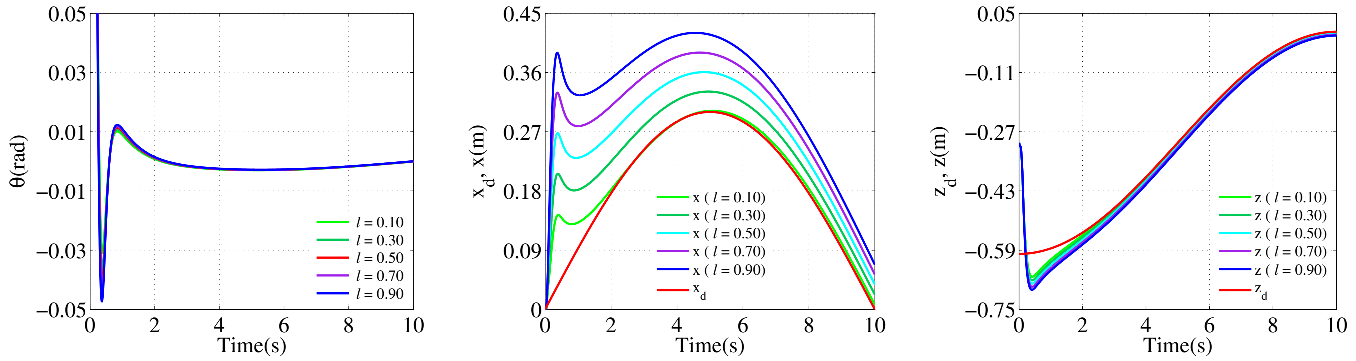

(**a**) (**b**) (**c**)

Figure 11. The simulation tests when $l = 0.10, 0.30, 0.50, 0.70$, and 0.90. (**a**) The θ; (**b**) the x_d and x; and (**c**) the z_d and z.

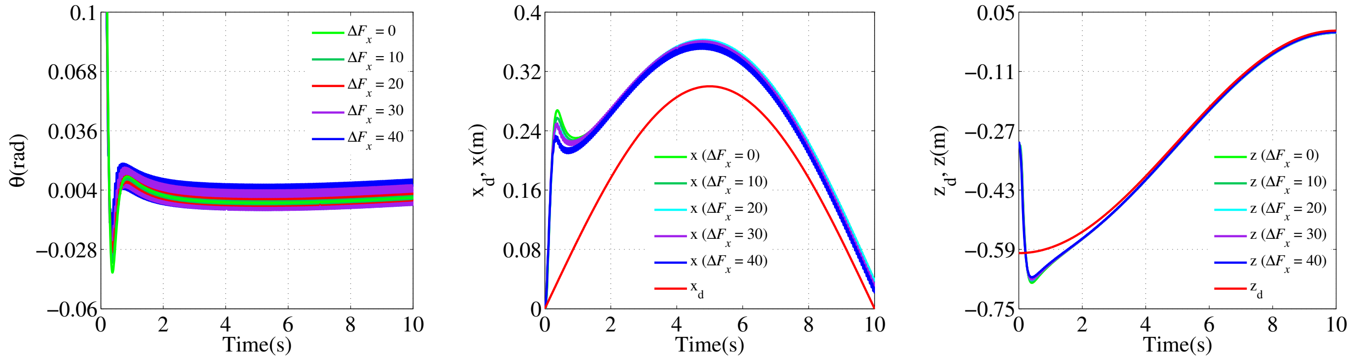

(**a**) (**b**) (**c**)

Figure 12. The simulation tests when $\Delta F_x = 0, 10, 20, 30$, and 40. (**a**) The θ; (**b**) the x_d and x; and (**c**) the z_d and z.

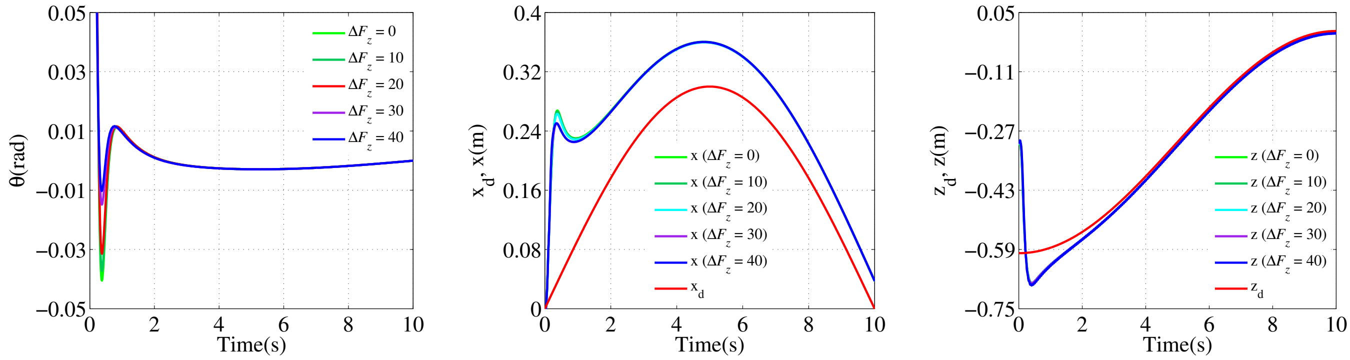

(**a**) (**b**) (**c**)

Figure 13. The simulation tests when $\Delta F_z = 0, 10, 20, 30$, and 40. (**a**) The θ; (**b**) the x_d and x; and (**c**) the z_d and z.

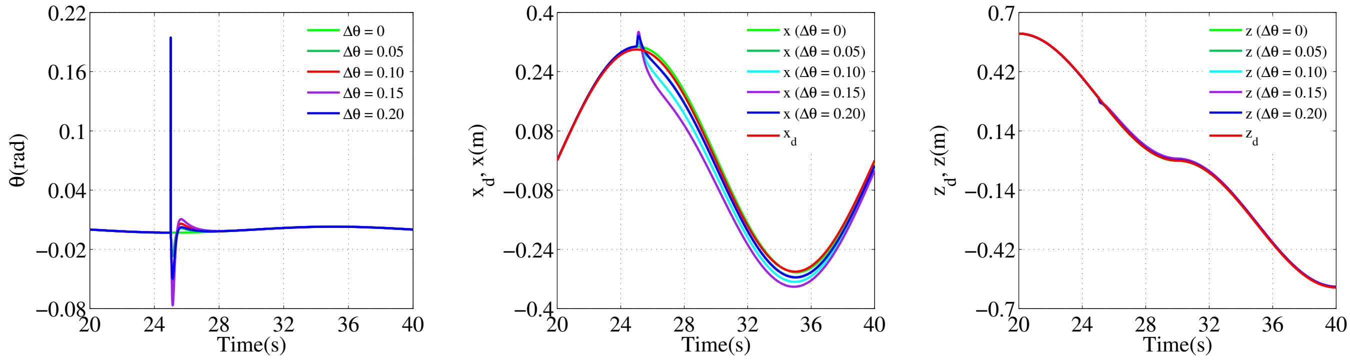

(**a**) (**b**) (**c**)

Figure 14. The simulation tests when $\Delta\theta = 0, 0.05, 0.10, 0.15$, and 0.20. (**a**) The θ; (**b**) the x_d and x; and (**c**) the z_d and z.

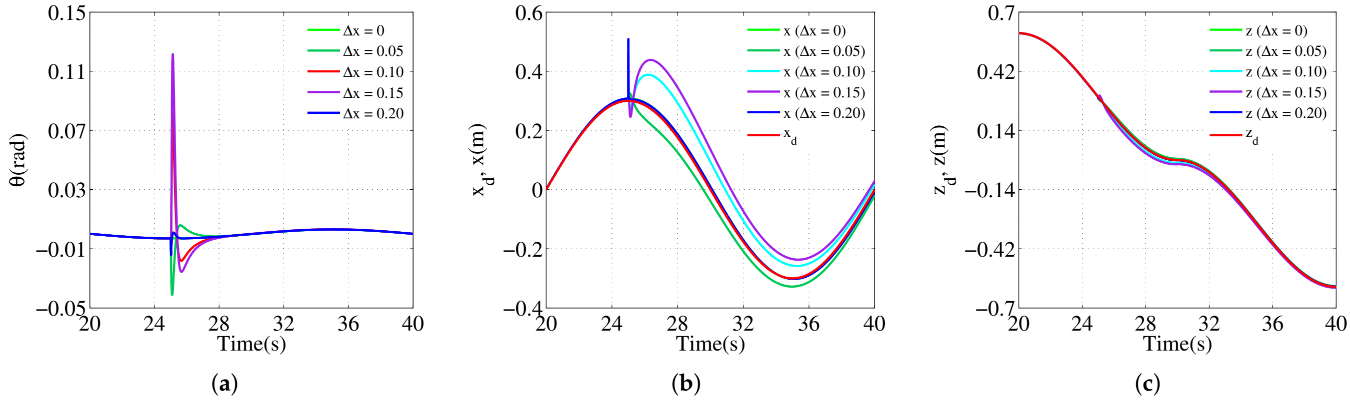

Figure 15. The simulation tests when $\Delta x = 0, 0.05, 0.10, 0.15$, and 0.20. (**a**) The θ; (**b**) the x_d and x; and (**c**) the z_d and z.

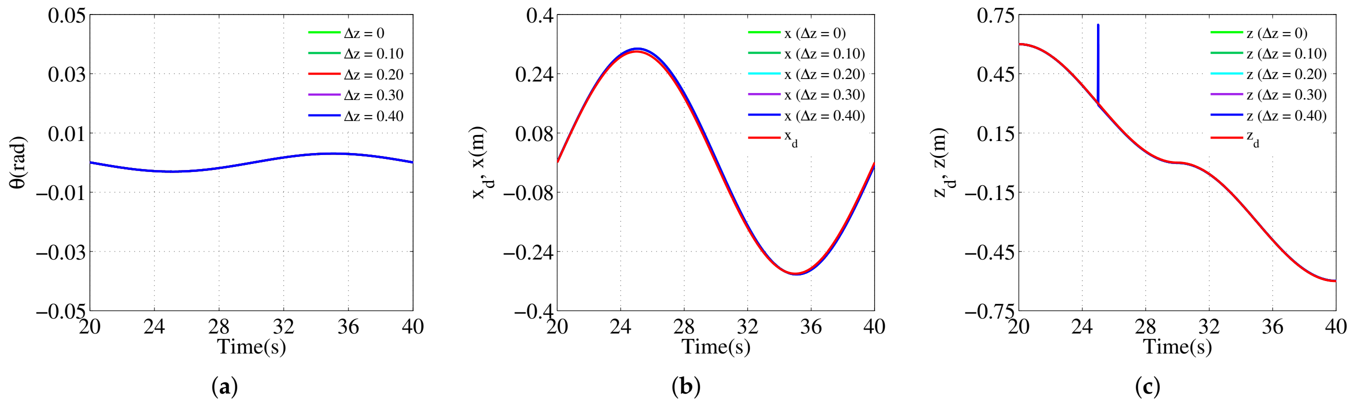

Figure 16. The simulation tests when $\Delta z = 0, 0.10, 0.20, 0.30$, and 0.40. (**a**) The θ; (**b**) the x_d and x; and (**c**) the z_d and z.

From the parameters design and the simulation results, we can obtain the following four conclusions.

(1) The proposed state and control variable transformation for the X-Z IP can reduce the difficulty of the controller design. Though the proposed transformation, the controller design becomes very easy.

(2) The proposed controller can make the X-Z IP track a trajectory in the vertical plane with good dynamic performance. The simulation results certify the rightness and effectiveness of the proposed block backstepping controller for the X-Z IP.

(3) The proposed controller has good robustness to system parameter uncertainties and external disturbances. The simulation results show that the control system can still reach a stable state when the system parameters change and external disturbances are added.

(4) In addition, the simulation results also prove that the decomposition of block model into reduced order model and zero dynamics is reasonable.

5. Discussions

Though the tracking control of the X-Z IP is achieved with the proposed controller, there still have three questions that need to be explained.

(1) The state transformation in (30) is a key transformation in the controller design. This transformation makes the controller design of v_1 and v_2 become easy, but this type of transformation make the stability proof of the state variables ξ_1, ξ_2, ξ_3, and ξ_4 become very complex. Then, other similar transformations can be tried to balance this design.

(2) In the computation of $\frac{df}{dt}$, three time derivative of the desired trajectory is required. This requirement is not strict generally. For the slow varying signal, three time differential can be omitted.

(3) In the state transformation and controller design, the state transformation and controller design is effective within a certain range of the parameter uncertainties and external disturbances.

6. Conclusions

This brief paper extended the research on the X-Z IP, and the tracking control of the X-Z IP was successfully achieved. The main contributions of this article can be concluded as following four aspects.

(1) A novel state transformation method was proposed for the X-Z IP. Through the state transformation, the model of the X-Z IP was transformed to simplified block model. The proposed transformation is very meaningful for the further research studies on the X-Z IP.

(2) The simplified block model was decomposed into reduced order model and zero dynamics. The block backstepping was deployed in the reduced order model. The control parameters can be selected to stabilize the zero dynamics.

(3) Simulation results were given to demonstrate the rightness and effectiveness of the proposed block backstepping controller in the tracking control of the X-Z IP.

(4) The proposed block backstepping controller for X-Z IP tracking control has good robustness to system parameter uncertainties and external disturbances.

Author Contributions: Conceptualization, J.-J.W.; methodology, J.-J.W. and Z.-Z.X.; software, J.-J.W. and Z.-Z.X.; validation, J.-J.W. and Z.-Z.X.; formal analysis, Z.-Z.X.; investigation, Z.-Z.X.; resources, J.-J.W.; data curation, Z.-Z.X.; writing—original draft preparation, J.-J.W. and Z.Z.X; writing—review and editing, Z.-Z.X. and J.-J.W.; visualization, Z.-Z.X.; supervision, J.-J.W.; project administration, J.-J.W.; funding acquisition, J.-J.W. All authors have read and agreed to the published version of the manuscript.

Funding: The work is supported by National Natural Science Foundation of China under Grant 61873079 and Key Research and Development Plan of Zhejiang Province of China under Grant 2021C03034.

Conflicts of Interest: The authors declare no conflict of interest.

References

1. Albouy, X.; Praly, L. On the use of dynamic invariants and forwarding for swinging up a spherical inverted pendulum. In Proceedings of the 39th IEEE Conference on Decision and Control, Sydney, Australia, 12–15 December 2000; pp. 1667–1672.
2. Bloch, A.M.; Leonard, N.E.; Marsden, J.E. Controlled Lagrangians and the stabilization of mechanical systems. I. The first matching theorem. *IEEE Trans. Autom. Control* **2000**, *45*, 2253–2270. [CrossRef]
3. Maravall, D. Control and stabilization of the inverted pendulum via vertical forces. In *Robotic Welding, Intelligence and Automation*; Springer: Berlin/Heidelberg, Germany, 2004; pp. 190–211.
4. Maravall, D.; Zhou, C.; Alonso, J. Hybrid fuzzy control of the inverted pendulum via vertical forces. *Int. J. Intell. Syst.* **2005**, *20*, 195–211. [CrossRef]
5. Astrom, K.J.; Furuta, K. Swinging up a pendulum by energy control. *Automatica* **2000**, *36*, 287–295. [CrossRef]
6. Shiriaev, A.S.; Egeland, O.; Ludvigsen, H.; Fradkov, A.L. VSS-version of energy-based control for swinging up a pendulum. *Syst. Control Lett.* **2001**, *44*, 45–56. [CrossRef]
7. Mason, P.; Broucke, M.; Piccoli, B. Time optimal swing-up of the planar pendulum. *IEEE Trans. Autom. Control* **2008**, 53, 1876–1886. [CrossRef]
8. Muskinja, N.; Tovornik, B. Swinging up and stabilization of a real inverted pendulum. *IEEE Trans. Ind. Electron.* **2006**, 53, 631–639. [CrossRef]
9. Angeli, D. Almost global stabilization of the inverted pendulum via continuous state feedback. *Automatica* **2001**, 37, 1103–1108. [CrossRef]
10. Liu, G.; Mareels, I.; Nesic, D. Decentralized control design of interconnected chains of integrators: A case study. *Automatica* **2008**, *44*, 2171–2178. [CrossRef]
11. Bloch, A.M.; Chang, D.E.; Leonard, N.E.; Marsden, J.E. Controlled Lagrangians and the stabilization of mechanical systems. II. Potential shaping. *IEEE Trans. Autom. Control* **2001**, *46*, 1556–1571. [CrossRef]
12. Srinivasan, B.; Huguenin, P.; Bonvin, D. Global stabilization of an inverted pendulum–control strategy and experimental verification. *Automatica* **2009**, *45*, 265–269. [CrossRef]
13. Wang, J.J.; Liu, D.L.; Wang, B.J. Research on one type of saturated nonlinear stabilization control method of X–Z inverted pendulum. *Acta Autom. Sin.* **2013**, *39*, 92–96. [CrossRef]

14. Lee, J.; Mukherjee, R.; Khalil, H.K. Output feedback stabilization of inverted pendulum on a cart in the presence of uncertainties. *Automatica* **2015**, *54*, 146–157. [CrossRef]
15. Liu, G.; Nesic, D.; Mareels, I. Non-linear stable inversion-based output tracking control for a spherical inverted pendulum. *Int. J. Control* **2008**, *81*, 116–133. [CrossRef]
16. Wang, J.J. Simulation studies of inverted pendulum based on PID controllers. *Simul. Model Pract. Theory* **2011**, *19*, 440–449. [CrossRef]
17. Wang, J.J. Stabilization and tracking control of X-Z inverted pendulum based on PID controllers. In Proceedings of the 2015 34th Chinese Control Conference (CCC), Hangzhou, China, 28–30 July 2015; pp. 4202–4207.
18. Wang, J.J. Stabilization and tracking control of X-Z inverted pendulum with sliding-mode control. *ISA Trans.* **2012**, *51*, 763–770. [CrossRef] [PubMed]
19. Pan, J.; Wang, Y. Stabilization and tracking control of X-Z inverted pendulum using flatness based active disturbance rejection control. *Asian J. Control* **2016**, *18*, 1714–1727. [CrossRef]
20. Kokotovic, P.V. The joy of feedback: Nonlinear and adaptive. *IEEE Control Syst. Mag.* **1992**, *12*, 7–17.
21. Krstic, M.; Kokotovic, P.V.; Kanellakopoulos, I. *Nonlinear and Adaptive Control Design*; Wiley Interscience: New York, NY, USA, 1995.
22. Chang, Y. Block backstepping control of MIMO systems. *IEEE Trans. Autom. Control* **2011**, *56*, 1191–1197. [CrossRef]
23. Rudra, S.; Barai, R.K.; Maitra, M. Nonlinear state feedback controller design for underactuated mechanical system: A modified block backstepping approach. *ISA Trans.* **2014**, *53*, 317–326. [CrossRef] [PubMed]
24. Rudra, S.; Barai, R.K.; Maitra, M. *Block Backstepping Design of Nonlinear State Feedback Control Law for Underactuated Mechanical Systems*; Springer: Singapore, 2017.
25. Isidori, A. The zero dynamics of a nonlinear system: From the origin to the latest progresses of a long successful story. *Eur. J. Control* **2013**, *19*, 369–378. [CrossRef]